# Design of an experimental apparatus for the performance evaluation of an active seat cushion system

Afonso Carvalho Martins
afonso.martins@tecnico.ulisboa.pt

Instituto Superior Técnico, Universidade de Lisboa, Portugal

June 2017

**Abstract**

This study is focused on the development of a semi-active cushion based on the concept proposed by the National Research Council of Canada with the objective of mitigating the vibrations felt by the aircrew of a helicopter in-flight. This semi-active cushion proposes the use of magnetorheological materials to vary the cushion's stiffness and damping properties. Samples of encapsulated magnetorheological fluids (MRF-Es) and magnetorheological elastomers (MREs) are developed and characterized to estimate its damping coefficient (MRF-Es) and elasticity and shear modulus (MREs) for different magnetic fields. In the MRE case, its performance is compared against commercial samples. The results shows that the MRF-Es damping coefficient and the MREs stiffness are highly dependent on the applied magnetic field. A cushion prototype is developed and manufactured. This cushion prototype has a modular design with nine cells that can be controlled independently. Preliminary tests show that its natural frequency is 21 Hz and that by applying a magnetic field the natural frequency can be increased to 28 Hz. By energizing the cells with MRF it is possible to verify that the resonance peak can be reduced by 70%.

**Keywords:** Semi-active vibration control, helicopter seat cushion, magnetorheological materials, material characterization, prototype development

## 1. Introduction

Helicopter vibrations are one of the helicopter's main problems as they are harmful for the aircrew's health, reduce the comfort and increase maintenance costs. These vibrations are mainly caused by the rotor blades as they suffer from asymmetrical loading that excite the cabin at N/rev harmonic frequencies [1]. Other sources of vibration include inertial loads, blade-vortex interactions and external interferences (i.e. gusts) that are conducted through the seat structure to the pilots, subjecting them to Whole Body Vibrations (WBV). The short term effects of the exposure to WBV include fatigue and lower back pain that although don't carry long term implications might cause distractions that can jeopardize the flight's mission. Truszczyska et al. [2] study reports that 70% of the interviewed pilots complained of lower back pain and 23% of them highlighted it as an impediment to fly the helicopter. Long term exposure to this type of vibration can lead so severe health issues like spinal misalignment and vibroacoustic disease (thickening of pericardial and arterial walls) [3].

The scientific community is committed on reducing the vibrations transmitted to the pilots in order to minimize the health risks and increase the comfort inside a helicopter.

This project is part of research partnership between the National Research Council of Canada (NRC) and the University of Victoria whose objective is to develop an adaptive seat cushion made with smart materials that can cancel the vibrations transmitted by the helicopter's cabin floor and that have the ability to adjust itself to different pilots and flight profiles.

## 2. Background

When a helicopter is flying it is subjected to high levels of structural vibration due to inertial and aerodynamic loads. These loads come from reactions to the blade passage, blade vortex interactions, blade stall, gusts, among others and vary with the maneuver that the helicopter is performing. Wickramasinghe [1] evaluated the effect of vibrations in a $50^{th}$ male percentile pilot and a $95^{th}$ percentile male co-pilot aboard of a Bell-412 helicopter and concluded that the vibration exposure felt by the co-pilot was superior to the pilot and that it was deemed "not safe" according to the ISO 2631 standard. These results show that is urgent to find effective ways to mitigate the vibration felt by a helicopter's aircrew.

## 2.1. Vibration Control Techniques

To reduce the vibrations caused by a helicopter, the research community have come up with different kind of solutions: passive, active and semi-active which can be applied to the rotor, the blades or to local components.

### 2.1.1 Passive solutions

Passive systems are the simplest solutions in terms of implementation to reduce helicopter vibrations. Due to the simplicity of these systems they can be described by sets of springs and dampers that are tuned in a way that the target excitation frequencies lies within the base isolation area of the system's transmissibility curve. These systems are cheap, easy to implement and can achieve relevant vibration reduction; however, since they need to be tuned for a specific frequency and do not have the ability to be tuned to adapt to different conditions [4, 1].

Chen et al. [5] evaluated a seat cushion prototype made with made with a combination of passive elements. This seat cushion was then tested in a Bell 412 helicopter with a $50^{th}$ percentile pilot and a $85^{th}$ percentile co-pilot and the results show that the cushion was more effective in mitigating vibrations for the co-pilot. This difference in performance visible just by swapping the operational conditions is the main drawback of passive solutions.

### 2.1.2 Active solutions

Active systems take advantage of actuators (pneumatic, hydraulic, piezoelectric, et cetera) to counteract the forces produced by the helicopter in the different stages of flight. The actuators can be placed on the rotor or blades or in specific points of the structure to reduce vibrations locally (seat mounts). These systems are controllable so they can be tuned according to certain performance parameters that can be maintained even if the operational scenarios change, however, they are complex and expensive systems, due to all sensors and actuators so they have high weight and power consumption penalties [6].

In a recent study Gan et al. [7] developed a system composed by a passive suspension to deal with the static load in parallel with two electromagnetic linear actuators that provide the active control authority over the structure. This prototype proved to be effective in canceling multiple harmonic frequencies in the low range spectrum (4 Hz - 12 Hz).

### 2.1.3 Semi-active solutions

Semi-active systems use materials with controllable properties to improve the general performance of the system. These materials have adjustable characteristics like variable damping or stiffness that are sensible to external stimuli and that allow to mitigate vibrations in different scenarios without the weight and power penalties of an active solution. The main drawback of semi-active systems is that their force range is limited so they can only be used to dampen vibrations locally.

The smart materials that are used in vibration control applications are usually magnetorheological materials, i.e. materials whose properties change in the presence of a magnetic field. Hiemenz et al. [8] retrofitted a magnetorheological damper in a SH-60 Seahawk helicopter seat and their results show that the incorporation of this device reduced 61% to 70% the most dominant harmonic felt by a $50^{th}$ percentile aviator when compared to the unmodified seat cushion.

## 2.2. Magnetorheological Materials

### 2.2.1 Magnetorheological Fluids

Magnetorheological Fluids (MRFs) were discovered by Jacob Rabinow at the U.S. National Bureau of Standards in the late 1940s. Although they presented several advantages in regard to its main competitor, the electroheological fluid, they also presented a non-predictable behavior due to thickening, sedimentation and abrasion problems that limited the potential of this technology. It was only in the 1990s that the MRFs started to be considered for applications mainly due to Lord Corporation's research and development [9].

The MRFs main components are a carrier fluid, usually water or oil, soft magnetic particles and additives to stabilize the mixture to prevent the problems mentioned above. When there is no applied magnetic field, the magnetic particles are suspended throughout the carrier fluid and it behaves like a Newtonian fluid; however, when a magnetic field is applied each magnetic particle becomes a dipole and is attracted to adjacent particles. In a matter of milliseconds, the magnetic particles form chains in the direction of the magnetic field changing the MRF from a liquid to a semi-solid state.

This material has three modes of operation: the flow mode, the shear mode and the squeeze mode. Several studies have been made to understand and predict the behavior of MRFs in squeeze mode: Farjoud et al. [10] introduced a mathematical model that assumes that the damping force is obtained by adding the pressure caused by the MRF's viscosity, inertia and MR effect. Guo et al. [11] developed a custom test rig where a small quantity of MRF is squeezed between two steel cylinders capable of supplying the samples with a uniform magnetic field. Using this test rig, Guo et al. registered a 132% increase in yield stress while increasing the applied magnetic field from 0.158 T to 0.28 T.

Despite the ability of providing a larger damping force with small amplitude displacements, using MRF dampers in squeeze mode has its disadvantages due to containment issues and a high dependence on the gap size between the two parallel plates. To overcome this containment issue, Wang et al. [12] developed a new MR composite where the MRF is encapsulated inside a regular elastomer pocket called Magnetorheological Fluid-Elastomer (MRF-E).

#### 2.2.2 Magnetorheological Elastomers

Another MR material used in vibration control are the Magnetorheological Elastomers (MREs). The MREs are composed by three main components: regular elastomer or another rubber-like material, magnetic particles and additives. During the manufacturing process, these components are mixed together to form a compound with the magnetic particles randomly dispersed in the mixture. Then, the mixture is cured, where the crosslinking between the elastomer molecules happens, and locks the magnetic particles in place. This process can be done without the presence of a magnetic field, which leads to an isotropic MRE, or while exposing the mixture to a strong magnetic field that causes the particles to become aligned with the magnetic field's direction, creating anisotropic MREs.

The MREs also have three modes of operation, the shear, the squeeze modes and the field-active mode where the MREs can change its shape due to the effect of the magnetic field in a process called magnetostriction [13].

The MREs present a field-depending elasticity and shear modulus instead of presenting a field-dependent viscosity and yield stress, like the MRFs, which make them cooperative instead of competing technologies [14]. This ability to control the shear and elasticity modulus allows to tune the stiffness of the system as is demonstrated in previous studies by Ginder et al. [15] that report a 24% increase in natural frequency.

The increasing use of MREs in commercial applications lead investigators to perform tests to optimize its performance: Jolly et al. [16] investigated the behavior of MREs with different magnetic particle concentrations and concluded that the optimal concentration is 30% (V/V); Lokander et al. [17] concluded that MREs with softer matrices have a higher relative MR effect; To use MREs in the aforementioned applications it is necessary to predict how they react under different loading amplitudes, frequencies and magnetic fields.

## 3. Prototype Conceptual Design

The figure 1 presents the conceptual design of the semi-active cushion proposed by the NRC [18]. This cushion should fit on a Bell-412 helicopter seat therefore its maximum dimensions have to be approximately 50 cm x 50 cm.

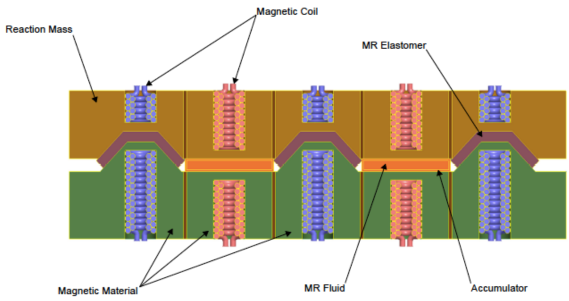


Figure 1: Semi-active cushion conceptual design [18]

Although not shown in figure 1, the cushion has a modular design where it is divided in 25 cells, each with 10 cm x 10 cm. Each cell has its own set of coils and MR materials (MRF or MRE) able to work independently from adjacent cells. In this conceptual design, the MRF is used in squeeze mode which is the most suitable mode of operation for a vibration control application with a very small stroke (under 1.5 mm). On the other cells, the MREs are inclined in regards to the applied force to engage them in shear and compression mode. It is assumed that the combination of these two operational modes provide a wider range of controllability over the variable stiffness properties of the MRE.

## 4. MR Materials Development and Characterization

This section includes the development and the characterization of the MR materials necessary to build the semi-active cushion.

### 4.1. MR Samples

#### 4.1.1 MRF-E samples

The developed MRF-E samples have two main elements, the MRF-140CG which is acquired from Lord Corporation and the regular elastomer used to encapsulate it, that is obtained from American Polyfilm Inc. This elastomer obtained is DT-2001 Thermoplastic Polyurethane (TPU), which is listed as having good compatibility with the MRF, and it is available in sheets with 10 and 20 mil thicknesses.

In order to manufacture the MRF-E samples, an aluminum mold with a hole and a hollow steel cylinder are manufactured. Then, a 20 mil sheet of TPU is placed on top of the mold and it is softened with a heat gun to gain a pocket with the mold form. Once it has cooled down, 4 ml of MRF are placed in the TPU pocket using a syringe and a sheet of 10 mil TPU is placed on top. The two are sealed together with the steel cylinder that is previously heated to a temperature of 160$^o$C.

### 4.1.2 MRE samples

The main objective of developing in-house MREs was manufacturing the softest MREs possible. This way, the elastomer chosen to be the MRE matrix is the Ecoflex 00-10 from Smooth-On Inc. that has a shore hardness of 00-10. The magnetic particles chosen are made from carbonyl iron powder and an additive is used to enhance the adhesion between the matrix and the magnetic particles. To fabricate the MRE samples, the magnetic particles were poured into a container. Then, 5 ml of the primer is added for 180 g of magnetic particles. The two components are mixed together and the mixture is left resting for 1 hour. Then, Ecoflex part A and Ecoflex part B are added to the mixture in a 1:1 ratio.After mixing the elastomer's part A and B, the cross-linking process begins and the pot-life of the mixture is 30 min therefore it has to be poured into the molds as quickly as possible.

4.2. Test Rigs

In order to characterize MR materials, the NRC provided its own custom rigs, one to test materials in shear and other in squeeze mode. Figures 2 and 3 shows the CAD models of these rigs with their main components highlighted.

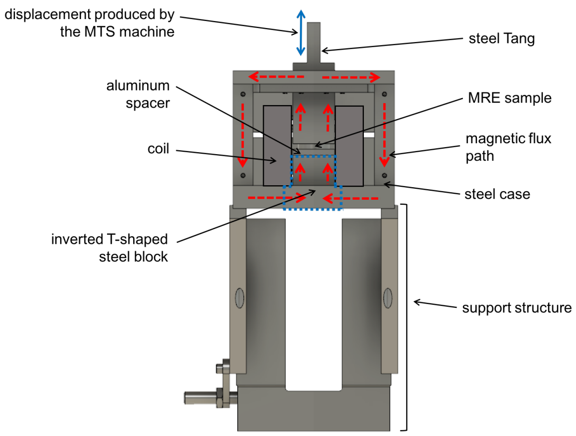


Figure 2: Compression test rig

The test rigs offer the capability of measuring the magnetic field that is applied to the samples in real-time. This means that reaching the target magnetic field is a matter of adjusting the current that is being supplied to the coils. This eliminates the need of

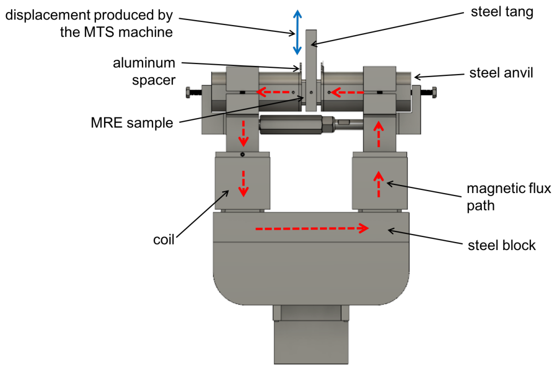


Figure 3: Shear test rig

relying on numerical analysis to calculate the current needed to provide the target magnetic field. The Hall effect sensor used in this study to measure the magnetic field is a model HGT-2010 from Lakeshore. To make sure that the Hall effect sensor measurements are accurate, the test rigs are analytically analyzed with Hopkinson's Law that relates the magnetomotive force produced by the coils with the magnetic flux going through the magnetic circuit.

The custom test rigs fit in a MTS 858 frame and are secured in place by two MTS 647 wedge grips. Figure 4 shows the experimental rigs fit in the MTS machine. The force is applied from the top of the frame by a hydraulic actuator and it measured at the bottom by a MTS 19F-03 force transducer.

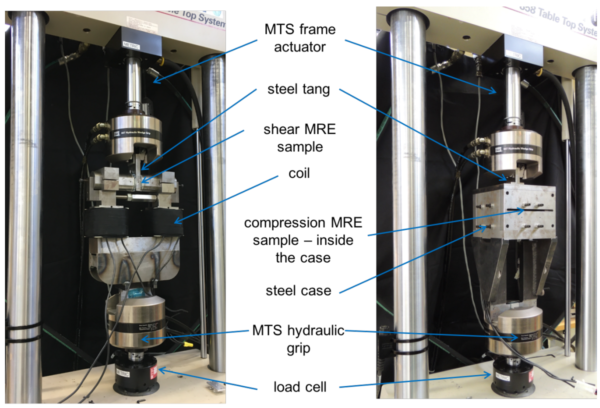


Figure 4: Experimental setup

4.3. Experimental Results

### 4.3.1 MRF-E

The experimental results shown below refer to tests made with the MRF-E samples that are cycled between displacements of $\pm$ 0.35 mm with loading frequencies of 1 Hz, 2.5 Hz, 5 Hz and 10 Hz and applied magnetic fields ranging from 0 T to 0.4 T in 0.1 T steps. The figure 5 presents an example of the hysteresis curves obtained for the tested MRFs cycled with a loading amplitude of ± 0.35 mm, a loading frequency of 1 Hz and various magnetic fields.

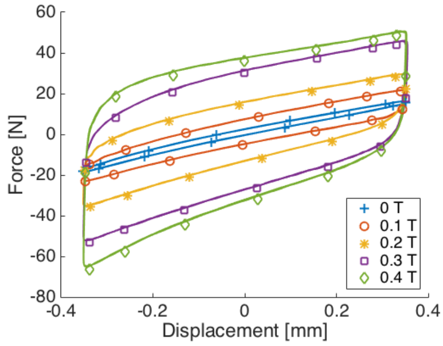


(a) MRF-140CG

Figure 5: Force-displacement curves for a sample with MRF-140CG

It is possible to conclude that the energy loss per cycle increases with the increase in the applied magnetic field as it is represented by the hysteresis area. This effect suggest that the damping properties of MRF-E sample are enhanced with the increase in applied magnetic field.

#### 4.3.2 MRE

#### 4.3.3 Shear mode

The MRE samples in shear mode are tested with loading strains of ± 1%, ± 2%, ± 3%, ± 4%, ± 5% and ± 10%, loading frequencies of 1 Hz, 2.5 Hz, 5 Hz and 10 Hz and applied magnetic fields up to 0.4 T. The figure 6 presents the stress-strain relationship obtained when cycling the sample with loading a strain of ± 2%, a loading frequency of 1 Hz and increasing magnetic field.

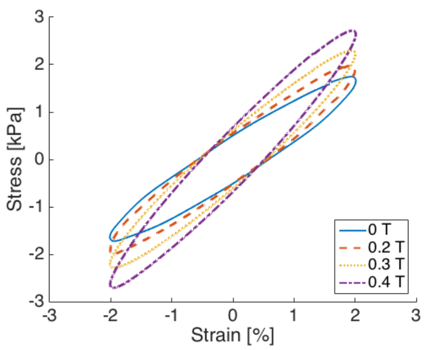


Figure 6: Stress-strain relationship for the in-house developed MRE in shear mode with a loading strain of ± 2%, a loading frequency of 1 Hz and varying magnetic field

The results show that with the increase in applied magnetic field the slope and area of the hysteresis curve increase with the increase in magnetic field. These increases are quantified by calculating the shear modulus and the loss factor for each of the applied magnetic fields and across the tested frequencies.

#### 4.3.4 Squeeze mode

In order to simulate the static load applied to the cushion when the pilot is seated, the MRE samples are subjected to a representative pre-strain of 11.5% . From this pre-strain value, the samples are subjected to strains of ± 2% with loading frequencies of 1 Hz, 2.5 Hz, 5 Hz and 10 Hz and applied magnetic fields varying from 0 T to 0.6 T in 0.1 T steps. Figure 7 presents the hysteresis curves obtained when cycling these samples at a frequency of 1 Hz for a pre-strain of 11.5%.

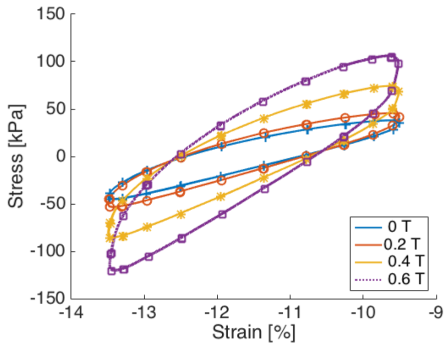


Figure 7: Hysteresis curves obtained when cycling the in-house developed samples in squeeze mode with the increase in applied magnetic field and a loading frequency of 1 Hz

The hysteresis curves in figure 7 show that the in-house developed MRE is highly influenced by the applied magnetic field. There is a noticeable change in the ellipsis slope and area which results in an increase in the elasticity modulus and in the energy dissipated by cycle.

## 5. Semi-Active Cushion

To facilitate the semi-active cushion certification process, the developed prototype have to fit in the existing seat frame of a Bell-412 helicopter which means that its maximum dimensions have to be 50 cm x 50 cm. Maintaining a modular design as the one shown in the conceptual design figure 1 and using the same coils as the ones used in the material characterization test rigs, nine cells fit in the available space. This conclusion is based on the assumption that each cell have its own coil so that the cells can work independently of each other. Figure

8 shows the disposition of the nine cells on the cushion. It is possible to verify in this preliminary drawing that the corners and the center of the cushion are populated with cells #2. The semi-active material inside these cells is MRE which means that they have variable stiffness. Note that It is intended that these cells provide as much stability and structure to the cushion as possible. The cells #1 fit into the available spaces between the cells #2 and provide variable damping to the structure. With this disposition, the cushion's MR materials are in parallel with each other therefore the total stiffness and damping coefficients of the cushion are the sum of the individual coefficients of each cell.

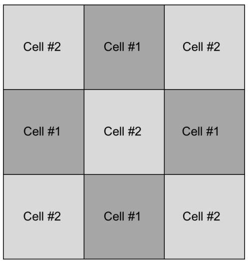


Figure 8: Preliminary cell disposition

5.1. Cells Preliminary Design

The design process of the semi-active cushion began with the decision of abandoning the idea of loading the MREs in mixed mode (load in shear and compression at the same time). In order for the MREs to work in mixed mode, the magnetic field has to excite the MRE samples in the same direction as the applied force. Designing a magnetic circuit that satisfied this condition would cause complications in the design and manufacturing processes.

There are several aspects of the design process that are common to both cells. The MR materials have to be in the vibration transmission path to have influence on the system. As a consequence, these materials have to support the pilot's weight as they are placed between the seat frame and the pilot. Also, to take the most advantage of the MR materials characteristics the cells need to be designed to conduct the highest magnetic field as possible. To maximize the cell's magnetic field, an iron core should be introduced inside the coil. This iron core, that should have the maximum cross-section area as possible and minimum length to minimize the reluctance, amplifies the magnetic field produced by the electromagnetic coils due to its steel high magnetic permeability. Note that air gaps lead to high magnetic losses so they should be avoided. Taking these guidelines in consideration, the plan is to place the MR material in the center of the cell and to make the two cells entirely of AISI 1018 steel which is known for its high magnetic permeability. Figure 9 present the preliminary drawing of cell #1, containing MRF-E and figure 10 shows the preliminary drawing of cell #2, containing MRE.

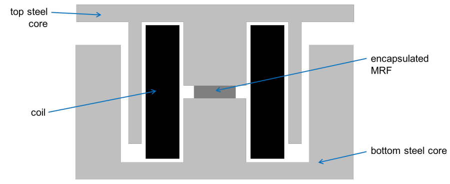


Figure 9: Cell #1, containing MRF-E preliminary design

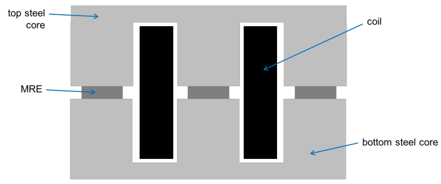


Figure 10: Cell #2, containing MRE preliminary design

Cell #1 is designed to have one encapsulated MRF specimen in its center. This posed a problem on how the magnetic circuit is to be closed at the exterior of the cell. The solution was to overlap the top and bottom steel parts so that the air gap remains minimal and constant when the cushion is operating. Since the MR materials have to sustain the static load, cell #2 allows for a higher amount of MR material to be used. In cell #2, a MRE specimen was placed in the center of the coil and a ring of MRE around the coil. With this configuration the air gaps between the two steel pieces are filled with MREs eliminating the need of the overlapped iron core strategy used in cell #1.

5.2. Cells Final Design

Figures 11 and 12 presents a 3D exploded view of the developed cell #1 and #2, with the main components highlighted.

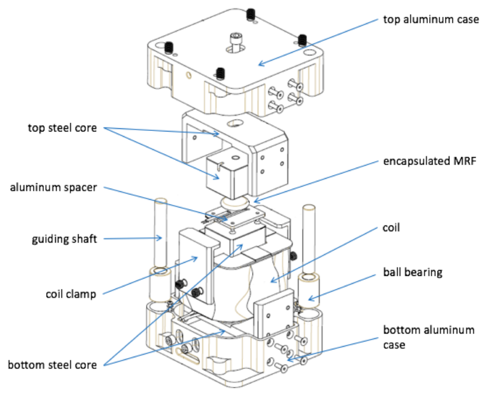


Figure 11: Cell #1

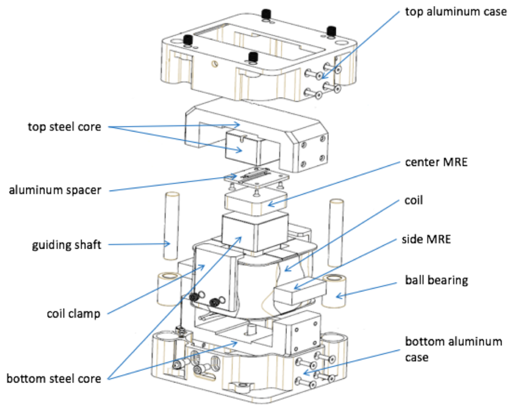


Figure 12: Cell #2

In accordance with the initial plan, the iron core would cover the entire extension of the cells (both the top and the bottom pieces) and these two pieces would overlap around the cell. With the weight reduction, the iron core that goes around the coil was limited to a strip with the width of the coil's center hole and a smaller thickness. With this modification, the two iron cores only overlap at two sides of the cells. The iron cores fit into two aluminum cases that hold the supporting structures that make the cells complete. The bottom aluminum case houses two clamps that secure the coil in place. A guiding system composed of two shafts and the corresponding ball bearings fits in the aluminum cases to ensure that the top and bottom pieces remain aligned at all times.

5.3. Assembled cushion

Figure 13 presents the exploded view of the assembled cushion with all nine cells. The configuration of the cells is the same as presented in the preliminary design, with 5 cells #2 in the center and corners and 4 cells #1 in between.

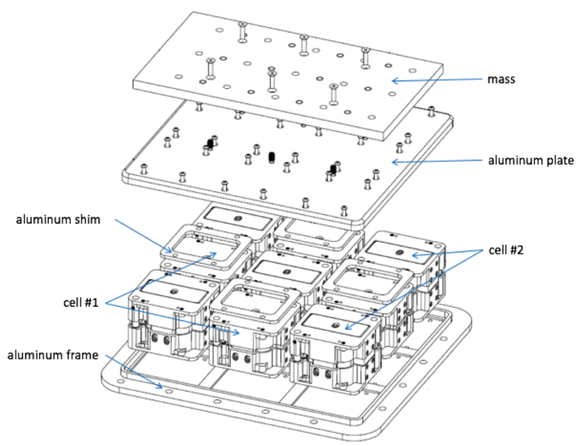


Figure 13: Assembly drawing

Figure 13 shows that the cells fit into an aluminum support frame and that they are covered by an aluminum plate where a payload mass can be mounted. In this setup the cells have a 2.5 cm gap between them to minimize any magnetic interference that could have existed between the cells. It is also worth mentioning that the encapsulated MRF specimens are unable to sustain the static load. To face this issue cells #1 have a smaller height than the cells #2. This way, when the mass is placed on the cushion, the structure will deflect without having an impact on the MRF specimen. Since it was hard to predict this static deflection in the design stage, a conservative approach was taken. The cushion was designed so that the top aluminum plate never touches cells #1 after the static deflection. The space between the cell and the aluminum plate is filled with aluminum shims whose thickness was set after measuring the gap.

Figure 14 shows the manufactured assembled cushion.

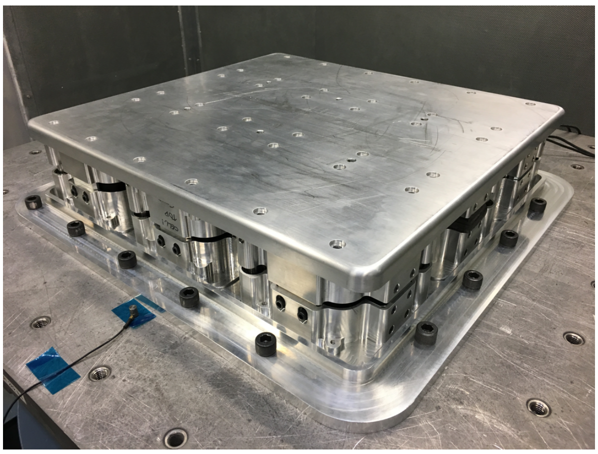

Figure 14: Semi-active cushion

5.4. Open Loop Tests

Open loop tests are performed on an assembly with three cells to investigate its ability to change its stiffness and damping properties. The figure 15 shows this experimental setup. The three cells are attached to the aluminum frame that is fixed to the shaker table and they are covered by the aluminum top plate. This shaker is a Unholtz-Dickie SA30-R16A electrodynamic shaker. The assembly is excited with a sine sweep from 80 Hz to 5 Hz at a rate of 0.5 Hz/s with a constant magnitude of 0.1 g. The mass on this setup is 70 lb.

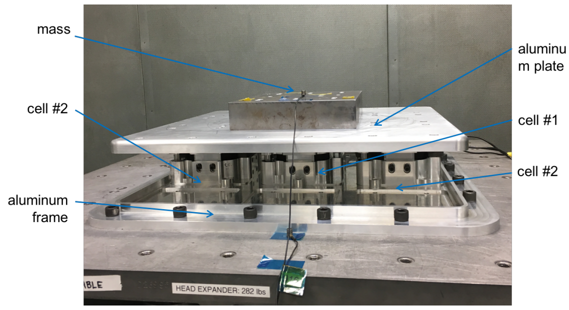


Figure 15: Assembly mounted on the shaker

The first open loop test made on this assembly evaluate the effect of varying its stiffness. To do so, DC currents ranging from 0 A to 5 A in 1 A steps are applied to the cells #2 and the resulting FRF magnitude and phase are plotted in figure 16.

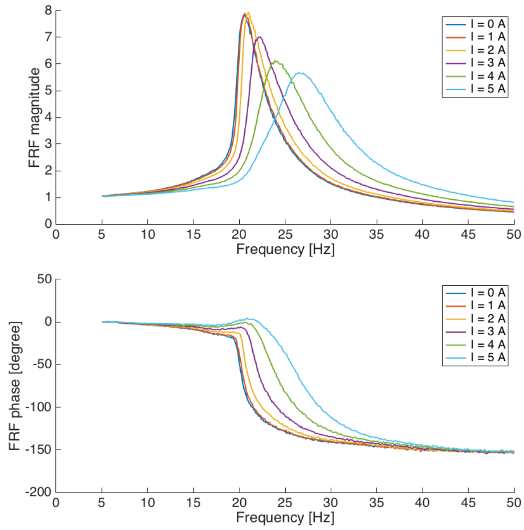


Figure 16: FRF magnitude and phase with the increase in stiffness

It is possible to observe that when the current is applied to cells #2 the system's natural frequency increases. This increase is a function of the applied magnetic field to the cells and for lower currents (below 2 A) its barely noticeable. For higher currents (above 2 A), the rate of the natural frequency increase is greater with the increase in applied current. Comparing the natural frequency at 0 A and 5 A it increases from 21 Hz to 28 Hz. These are encouraging results because they prove that the cell's #2 have the ability to control the natural frequency of the cushion. These open loop tests also show that the magnitude of the FRF decreases when the current increases denoting an increase in the cell's damping properties.

The second open loop test has the objective of verifying if the damping properties of the cell #1 are enhanced with the application of magnetic field. To do so, the assembly's cell #1 is subjected to DC currents of 0 A, 1 A, 2 A and 3 A. The FRF's magnitude and phase are presented in figure 17.

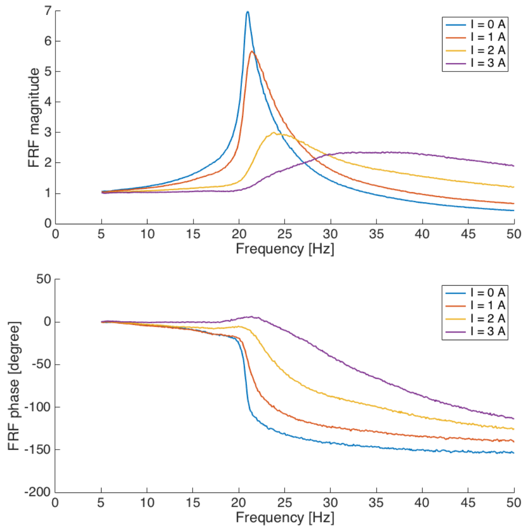


Figure 17: FRF magnitude and phase with the increase in damping

The results are, once again, according to what is expected. The increase in applied current increases the damping properties of this assembly as the magnitude of the FRF decreases approximately 70%. The disadvantage of increasing the damping coefficient of a structure without any type of control is patent on figure 17 as the magnitude of the higher frequency excitation increases with the increase in applied current.

## 6. Conclusions

A semi-active cushion prototype was developed based on a conceptual design. This cushion relies on magnetorheological materials to mitigate vibrations produced by a helicopter. It was necessary to develop and characterize samples of these materials in order to predict how would they perform when incorporated in the cushion. The first material that was developed was the MRF-E. The test results showed that the sample's damping coefficient increased with the increase in the applied magnetic field strength.The second material tested was the in-house developed MRE where all of its components were selected with the purpose of ensuring a soft composite with the highest MR effect possible. This material was tested in shear and in squeeze mode and the results showed a 53% and 178% increase in shear and elasticity modulus, respectively.

The final section of this study presented the design process of the developed semi-active cushion and the preliminary tests done on the prototype. This prototype features a modular design with nine cells where five include MREs and the other four MRF-Es. Several open loop tests are realized. In these tests, an assembly composed by three cells was excited with DC current to evaluate if the cells had the ability of changing the stiffness and the damping of the assembly. These tests were promising as it was possible to change the natural frequency of the assembly from 21 Hz to 28 Hz and reduce the magnitude of the resonance response in 70% when exciting the cells with variable stiffness and damping, respectively.

## References


[1] Viresh Kanchana Wickramasinghe. *Dynamics Control Approaches to Improve Vibratory Environment of the Helicopter Aircrew*. PhD thesis, Carleton University Ottawa, 2012.

[2] Aleksandra Truszczynska, Rafal Lewkowicz, Olaf Truszczynski, Kazimierz Rapala, and Mieczyslaw Wojtkowiak. Back pain in polish military helicopter pilots. *International journal of occupational medicine and environmental health*, 25(3):258–264, 2012.

[3] Branco NA Castelo and E Rodriguez. The vibroacoustic disease–an emerging pathology. *Aviation, space, and environmental medicine*, 70(3 Pt 2):A1–6, 1999.

[4] Kenneth B Amer and James R Neff. Vertical-plane pendulum absorbers for minimizing helicopter vibratory loads. *Journal of the American helicopter Society*, 19(4):44–48, 1974.

[5] Y. Chen, Viresh Wickramasinghe, and D. Zimcik. Flight test of prototype seat cushion performance for helicopter aircrew whole-body vibration mitigation. Technical Report LTR-FRL-2013-0033, National Research Council Canada, 2013.

[6] John T. Pearson. *Adaptive strategies for the active control of helicopter vibration*. PhD thesis, Loughborough University, United Kingdom, 1994.

[7] Zengkang Gan, Andrew J Hillis, and Jocelyn Darling. Adaptive control of an active seat for occupant vibration reduction. *Journal of Sound and Vibration*, 349:39–55, 2015.

[8] Gregory J Hiemenz, Wei Hu, and Norman M Wereley. Semi-active magnetorheological helicopter crew seat suspension for vibration isolation. *Journal of Aircraft*, 45(3):945–953, 2008.

[9] Mark R Jolly, Jonathan W Bender, and J David Carlson. Properties and applications of commercial magnetorheological fluids. *Journal of Intelligent Material Systems and Structures*, 10(1):5–13, 1999.

[10] Alireza Farjoud, Ryan Cavey, Mehdi Ahmadian, and Michael Craft. Magneto-rheological fluid behavior in squeeze mode. *Smart Materials and Structures*, 18(9):095001, 2009.

[11] Chaoyang Guo, Xinglong Gong, Shouhu Xuan, Qifan Yan, and Xiaohui Ruan. Squeeze behavior of magnetorheological fluids under constant volume and uniform magnetic field. *Smart Materials and Structures*, 22(4):045020, 2013.

[12] Xiaojie Wang, Faramarz Gordaninejad, and Gregory H Hitchcock. Dynamic behaviors of magnetorheological fluid-elastomer composites under oscillatory compression. In *Smart Structures and Materials*, pages 250–258. International Society for Optics and Photonics, 2004.

[13] Yancheng Li, Jianchun Li, Weihua Li, and Haiping Du. A state-of-the-art review on magnetorheological elastomer devices. *Smart materials and structures*, 23(12):123001, 2014.

[14] Marke Kallio. *The elastic and damping properties of magnetorheological elastomers*. VTT, 2005.

[15] John M Ginder, William F Schlotter, and Mark E Nichols. Magnetorheological elastomers in tunable vibration absorbers. In *SPIE's 8th Annual International Symposium on Smart Structures and Materials*, pages 103–110. International Society for Optics and Photonics, 2001.

[16] Mark R Jolly, J David Carlson, and Beth C Munoz. A model of the behaviour of magnetorheological materials. *Smart Materials and Structures*, 5(5):607, 1996.

[17] Mattias Lokander and Bengt Stenberg. Performance of isotropic magnetorheological rubber materials. *Polymer Testing*, 22(3):245–251, 2003.

[18] Amin Fereidooni. Semi-active control of helicopter seat cushion: Controllable cushion layer (ccl). Technical Report LM-FRL-2015-0035, National Research Council of Canada, Jul 2015.